JACS
JOURNAL OF THE AMERICAN CHEMICAL SOCIETY

Subscriber access provided by ISTANBUL TEKNIK UNIV

Article

Self-delivering Nanoemulsions for Dual Fluorine-19 MRI and Fluorescence Detection

Jelena M. Janjic, Mangala Srinivas, Deepak K. K. Kadayakkara, and Eric T. Ahrens

J. Am. Chem. Soc., **2008**, 130 (9), 2832-2841 • DOI: 10.1021/ja077388j

Downloaded from http://pubs.acs.org on February 8, 2009

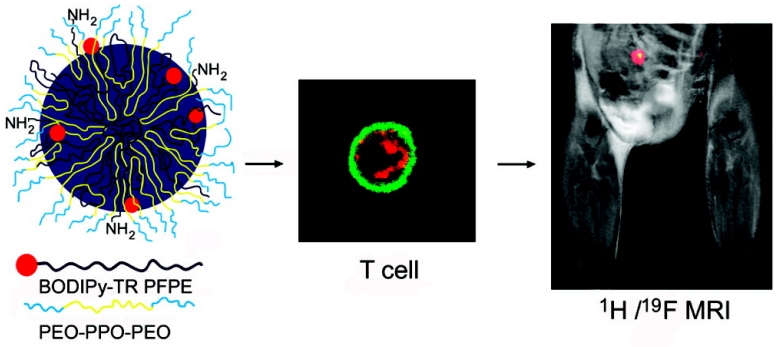

More About This Article

Additional resources and features associated with this article are available within the HTML version:

- Supporting Information
- Links to the 2 articles that cite this article, as of the time of this article download
- Access to high resolution figures
- Links to articles and content related to this article
- Copyright permission to reproduce figures and/or text from this article

View the Full Text HTML

ACS Publications
High quality. High impact.

Journal of the American Chemical Society is published by the American Chemical Society. 1155 Sixteenth Street N.W., Washington, DC 20036

J|A|C|S
ARTICLES
Published on Web 02/12/2008

Self-delivering Nanoemulsions for Dual Fluorine-19 MRI and Fluorescence Detection

Jelena M. Janjic, Mangala Srinivas, Deepak K. K. Kadayakkara, and Eric T. Ahrens*

Department of Biological Sciences and Pittsburgh NMR Center for Biomedical Research, Carnegie Mellon University, 4400 Fifth Ave., Pittsburgh, Pennsylvania 15213

Received September 26, 2007; E-mail: eta@andrew.cmu.edu

Abstract: We report the design, synthesis, and biological testing of highly stable, nontoxic perfluoropolyether (PFPE) nanoemulsions for dual ^{19}F MRI-fluorescence detection. A linear PFPE polymer was covalently conjugated to common fluorescent dyes (FITC, Alexa647 and BODIPy-TR), mixed with pluronic F68 and linear polyethyleneimine (PEI), and emulsified by microfluidization. Prepared nanoemulsions (<200 nm) were readily taken up by both phagocytic and non-phagocytic cells in vitro after a short (~3 h) co-incubation. Following cell administration in vivo, ^{19}F MRI selectively visualizes cell migration. Exemplary in vivo MRI images are presented of T cells labeled with a dual-mode nanoemulsion in a BALB/c mouse. Fluorescence detection enables fluorescent microscopy and FACS analysis of labeled cells, as demonstrated in several immune cell types including Jurkat cells, primary T cells and dendritic cells. The intracellular fluorescence signal is directly proportional to the ^{19}F NMR signal and can be used to calibrate cell loading in vitro.

Introduction

The persistence of complex medical conditions, such as autoimmune diseases, cancers, and neurodegenerative diseases, is prompting the development of cellular therapies. Cell therapy is used to stimulate or re-program the immune system or regenerate damaged tissues. Therapeutic cells are selected, multiplied, and pharmacologically treated ex vivo and then transferred into the body. Cell populations, such as stem cells[1−4] or various immune cell types [e.g., natural killer cells,[5] dendritic cells (DCs)[6−8] and T cells[9]] are frequent vehicles for these therapies. However, a major obstacle in cell therapy is the lack of a reliable, noninvasive method for determining the quantity of therapeutic cells present in the target tissue in vivo. Additionally, there is a diagnostic need to noninvasively visualize sites of innate inflammatory response due to lesions, cancer progression and metastases,[10] or organ transplant rejection[11] by tracking specific immune cell populations in vivo.

MRI is emerging as a modality for noninvasive cell tracking in vivo.[12−14] Conventionally, paramagnetic contrast agents, such as superparamagnetic iron oxide (SPIO) nanoparticles, are employed to label cells of interest either ex vivo or in situ.[15] Paramagnetic agents modulate the NMR relaxation times (i.e., T_1, T_2, and/or T_2*) of labeled cells, thus providing image contrast in conventional ^{1}H images.[16] Often, however, these contrast changes can be challenging to unambiguously identify and interpret. Furthermore, quantification of the number of labeled cells in image regions of interest is experimentally complex.[17]

Recently, a novel imaging platform relying on ^{19}F MRI of perfluorocarbon-labeled cells has been described.[18,19] In this approach for cellular imaging, therapeutic or diagnostic cells are labeled ex vivo with the perfluorocarbon nanoparticles, labeled cells are introduced into a subject, and cell trafficking is monitored in vivo using ^{19}F MRI.[18−20] The low biological abundance of ^{19}F in tissues yields background-free images and provides a means for highly selective detection of labeled cells in vivo throughout the organism. Perfluorocarbons are attractive compounds for formulating ^{19}F MRI reagents due to their biological and chemical inertness. In fact, perfluorocarbons have been used clinically as blood substitutes since the early 1980s because of their high gas dissolving capacity for oxygen and

(1) Beeres, S. L. M. A.; Bengel, F. M.; Bartunek, J.; Atsma, D. E.; Hill, J. M.; Vanderheyden, M.; Penicka, M.; Schalij, M. J.; Wijns, W.; Bax, J. J. *J. Am. Coll. Cardiol.* **2007**, *49*, 1137−1148.
(2) Hoshino, K.; Ly, H. Q.; Frangioni, J. V.; Hajjar, R. J. *Prog. Cardiovasc. Dis.* **2007**, *49*, 414−420.
(3) Ittrich, H.; Lange, C.; Togel, F.; Zander, A. R.; Dahnke, H.; Westenfelder, C.; Adam, G.; Nolte-Ernsting, C. *J. Magn. Reson. Imaging* **2007**, *25*, 1179−1191.
(4) Mimeault, M.; Hauke, R.; Batra, S. K. *Clin. Pharmacol. Ther.* **2007**, *82*, 252−264
(5) Ljunggren, H. G.; Malmberg, K. J. *Nat. Rev. Immunol.* **2007**, *7*, 329−339.
(6) Villadangos, J. A.; Schnorrer, P. *Nat. Rev. Immunol.* **2007**, *7*, 543−555.
(7) Zhong, H.; Shurin, M. R.; Han, B. *Exp. Rev. Vacc.* **2007**, *6*, 333−345.
(8) Akbar, F.; Abe, M.; Yoshida, O.; Murakami, H.; Onji, M. *Curr. Med. Chem.* **2006**, *13*, 3113−3119.
(9) June, C. H. *J. Clin. Invest.* **2007**, *117*, 1466−1476.
(10) Karin, M.; Greten, F. R. *Nat. Rev. Immunol.* **2005**, *5*, 749−759.
(11) Ho, C.; Hitchens, T. K. *Curr. Pharm. Biotechnol.* **2004**, *5*, 551−566.
(12) Gilad, A. A.; Winnard, P. T., Jr.; van Zijl, P. C. M.; Bulte, J. W. M. *NMR Biomed.* **2007**, *20*, 275−290.
(13) Corot, C.; Robert, P.; Ideé, J. M.; Port, M. *Adv. Drug Delivery Rev.* **2006**, *58*, 1471−1504.
(14) Frank, J. A.; Anderson, S. A.; Kalsih, H.; Jordan, E. K.; Lewis, B. K.; Yocum, G. T.; Arbab, A. S. *Cytotherapy* **2004**, *6*, 621−625.
(15) Bulte, J. W. M.; Kraitchman, D. L. *NMR Biomed.* **2004**, *17*, 484−499.
(16) Arbab, A. S.; Liu, W.; Frank, J. A. *Exp. Rev. Med. Devices* **2006**, *3*, 427−439.
(17) Verdijk, P.; Scheenen, T. W. J.; Lesterhuis, W. J.; Gambarota, G.; Veltien, A. A.; Walczak, P.; Scharenborg, N. M.; Bulte, J. W. M.; Punt, C. J. A.; Heerschap, A.; Figdor, C. G.; De Vries, I. J. M. *Int. J. Cancer* **2007**, *120*, 978−984.
(18) Ahrens, E. T.; Flores, R.; Xu, H. Y.; Morel, P. A. *Nat. Biotechnol.* **2005**, *23*, 983−987.
(19) Srinivas, M.; Morel, P. A.; Ernst, L. A.; Laidlaw, D. H.; Ahrens, E. T. *Magn. Reson. Med.* **2007**, *58*, 725−734.
(20) Ahrens, E. T. 2005, WO 2005/072780 A2.

 10.1021/ja077388j CCC: $40.75 **© 2008 American Chemical Society**

Scheme 1. Synthesis of PFPE Amides from PFPE Ester.

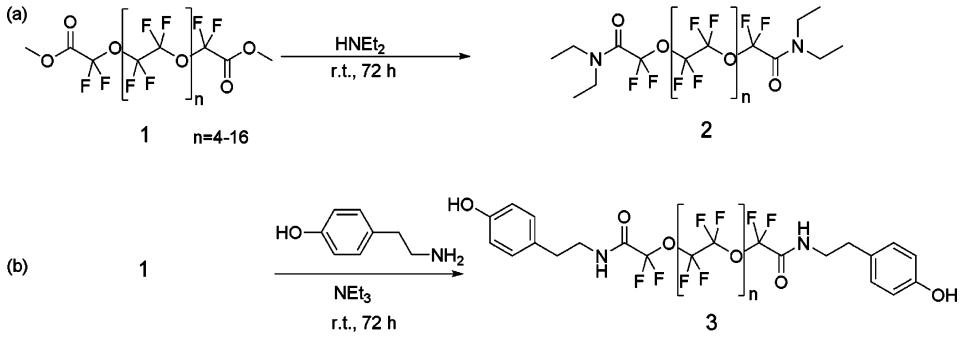

carbon-dioxide, and chemical and metabolic stability.[21] Symmetric perfluoropolyethers (PFPEs), particularly linear and macrocyclic structures,[22−27] are attractive fluorocarbons for ^{19}F MRI reagent development; the simplicity of their ^{19}F NMR spectra and a high number of NMR-equivalent nuclei (>20) yields high ^{19}F MRI sensitivity.[22,23]

In vivo ^{19}F MRI cell tracking is often not sufficient to follow cellular fate and cellular phenotype post-transfer. A dual fluorescent-MRI cellular labeling reagent is highly desirable for recovery and further study of cells post-imaging. The fluorescent moiety facilitates unambiguous identification and recovery of labeled cells from tissues. Fluorescence-based detection techniques (e.g., microscopy and immunocytochemistry) can provide confirmation of the MRI cell tracking results in bioposied tissues. Using, for example, fluorescence activated cell sorting (FACS) analysis, one can elucidate any phenotypic changes of the labeled cells or identify possible in vivo transfer of the label to other cell types (e.g., macrophages).

In this paper, we report the design and synthesis of a novel nanoemulsion of a mean particle size of 160−190 nm that enables both ^{19}F MRI cell tracking and fluorescence-based detection. This nanoemulsion-based agent can efficiently enter and label a wide range of cell types in culture, including nonphagocytic cells. The fluorescent moiety is directly conjugated to the ^{19}F MRI PFPE tracer, making it a true dual-mode reagent. The synthetic procedures reported here are simple and easily scalable. Our synthetic methodology exploits high reactivity of PFPE alkyl esters to the nucleophilic attack by primary or secondary amines. PFPE esters readily couple directly to amines without the need for further activation of the carbonyl.[28] Resulting secondary or tertiary PFPE amides are sufficiently stable to allow further processing into nanoemulsion by microfluidization. The direct conjugation solves the problem of differential distribution of the fluorescent dye and the MRI label in tissues, which may occur if the two are merely co-emulsified. Previous studies[18,29,30] add a lypophilic dye to the surfactant mixture for fluorescence detection. However, this approach is less robust than a direct conjugation approach because lypophilic dyes have a tendency to dissolve and distribute in cell membranes they come in contact with, potentially leading to nonspecific fluorescent cell labeling in vivo. We show that our dual mode reagent can efficiently label T cells and DCs in culture and is nontoxic. A linear correlation between the ^{19}F NMR signal and the fluorescence signal is observed in both free nanoemulsion and in labeled cells. We also show in vivo ^{19}F MRI results that track labeled T cells transferred into a mouse model. Following the in vivo imaging, fluorescence microscopy and FACS analysis were performed on the labeled T cells. Our results suggest that dual-mode ^{19}F MRI-fluorescence nanoemulsions are powerful cellular imaging reagents that can be used to label a wide range of cell types in support of discovery and preclinical animal studies.

Results

1. Fluorescent PFPE Nanoemulsions. 1.1. Synthesis of PFPE Amides. PFPE methyl ester 1 (Exfluor Inc. Inc., TX) was used as the starting material for all reported PFPE derivatives, including fluorescent blended PFPE amide (FBPA). PFPE methyl ester is a mixture of oligomers represented by a formula $CH_3O(O)CCF_2O(CF_2CF_2O)_nCF_2$ $C(O)OCH_3$, where $n = 4-16$, and the average molecular weight is 1750 g/mol. PFPE esters can easily react with primary and secondary amines without additional ester activation, due to the increased nucleophilicity of the carbonyl by the electron withdrawing effect of neighboring fluorines.[28] In general, PFPE methyl ester 1 was mixed with excess primary or secondary amine, either as a neat liquid or a solution of the amine in an appropriate solvent, under inert atmosphere (Scheme 1a). The reaction mixture was allowed to stir for 72 h at r.t. Reaction progress was monitored by ^{1}H NMR. After the reaction was complete, high vacuum was employed to remove the side product methanol and the excess of unreacted amine. PFPE amide derivative purification was performed using a recently published method for purification of linear PFPEs by selective organic solvent extractions.[31]

When organic solvent extraction was not sufficient, adsorption to fluorous silica gel and elution of the purified product with methanol followed by trifluorothanol or perfluorohexanes was used.[32] Structures of the PFPE amide derivatives were confirmed

(21) Spahn, D.; Kocian, R. *Curr. Pharm. Des.* **2005**, *11*, 4099−4114.
(22) Helmer, K. G.; Han, S.; Sotak, C. H. *NMR Biomed.* **1998**, *11*, 120−130.
(23) Dardzinski, B. J.; Sotak, C. H. *Magn. Reson. Med.* **1994**, *32*, 88−97.
(24) McNab, J. A.; Yung, A. C.; Kozlowski, P. *Magn. Reson. Mater. Phys., Biol., Med.* **2004**, *17*, 288−295.
(25) Nöth, U.; Rodrigues, L. M.; Robinson, S. P.; Jork, A.; Zimmermann, U.; Newell, B.; Griffiths, J. R. *Int. J. Radiat. Oncol., Biol., Phys.* **2004**, *60*, 909−919.
(26) Fan, X.; River, J. N.; Zamora, M.; Al-Hallaq, H. A.; Karczmar, G. S. *Int. J. Radiat. Oncol., Biol., Phys.* **2002**, *54*, 1202−1209.
(27) Nöth, U.; Morrissey, S. P.; Deichmann, R.; Jung, S.; Adolf, H.; Haase, A.; Lutz, J. *Artif. Cells Blood Substit. Immobil. Biotechnol.* **1997**, *25*, 243−254.
(28) Tonelli, C.; Gavezotti, P.; Strepparola, E. *J. Fluorine Chem.* **1999**, *95*, 51−70.
(29) Caruthers, S. D.; Neubauer, A. M.; Hockett, F. D.; Lamerichs, R.; Winter, P. M.; Scott, M. J.; Gaffney, P. J.; Wickline, S. A.; Lanza, G. M. *Invest. Radiol.* **2006**, *41*, 305−312.
(30) Partlow, K. C.; Chen, J.; Brant, J. A.; Neubauer, A. M.; Meyerrose, T. E.; Creer, M. H.; Nolta, J. A.; Caruthers, S. D.; Lanza, G. M.; Wickline, S. A. *FASEB J.* **2007**, *21*, 1647−54.
(31) Burns, J. M. **2006**. USP 7038068.
(32) Zhang, W.; Curran, D. P. *Tetrahedron* **2006**, *62*, 11837−11865.

Scheme 2. Synthesis of FBPAs[a]

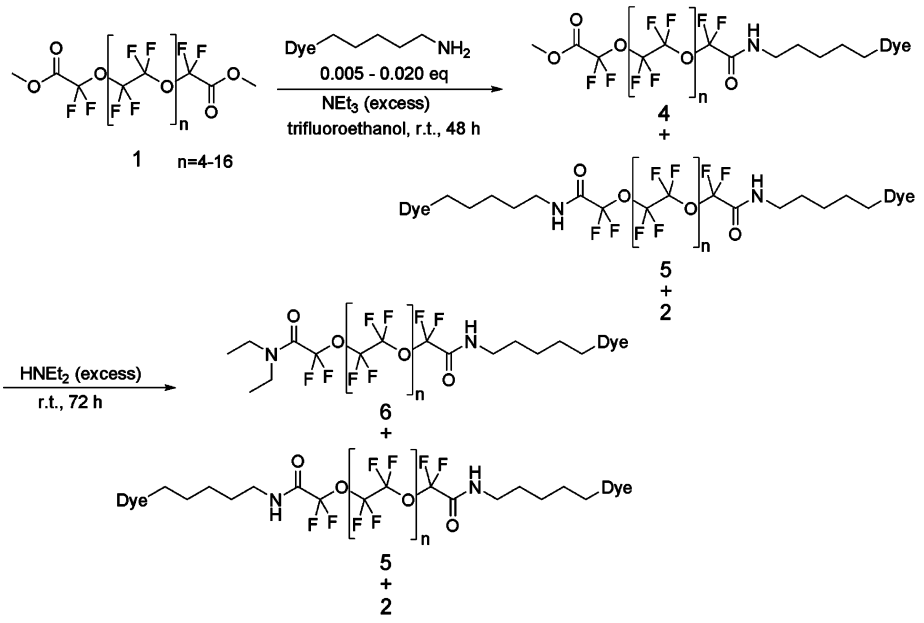

[a] Fluorescent blended PFPE amide (FBPA) is a mixture of PFPE derivatives 2, 5 and 6, where "Dye" is BODIPy-TR, FITC, or Alexa647.

Chart 1. Fluorescent PFPE Nanoemulsion Components. "Dye" is BODIPy-TR, FITC, or Alexa647.

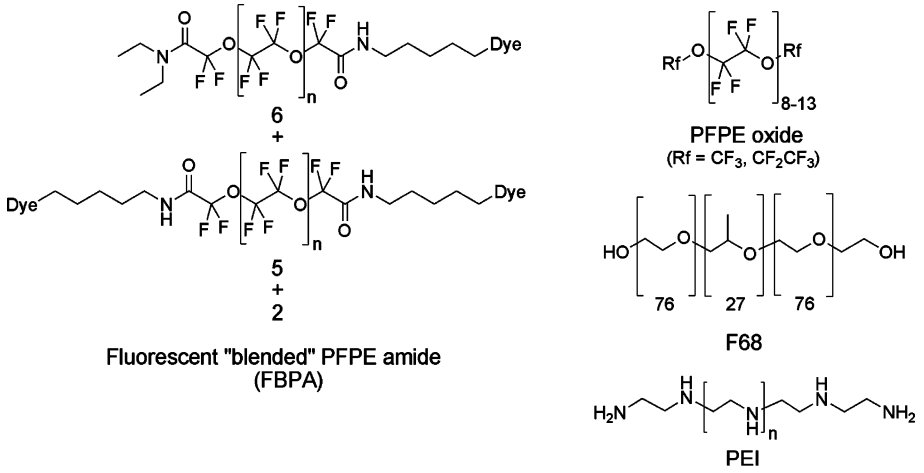

by ^{1}H and ^{19}F NMR. PFPE amide synthesis is easily scalable, and we have successfully prepared up to 50 g of PFPE amide 2 and 15 g of PFPE amide 3.

Preparation of PFPE amide 3 served as a model reaction for coupling nonvolatile primary amines to PFPE ester 1; we used 4-(2-aminoethyl) phenol as a model primary amine (Scheme 1b). The amine suspended in chloroform was added to PFPE ester 1 in the presence of excess triethylamine under inert atmosphere. The reaction was stirred at room temperature for 72 h. The final product PFPE amide 3 was purified by fluorous solid-phase extraction. The reaction was also tested in trifluoroethanol as a solvent, and complete conversion (>99% by ^{1}H NMR) of the PFPE ester end groups to PFPE secondary amides was observed after 48 h (data not shown). The high reactivity of PFPE esters to primary amines allows complete ester to amide conversion at room temperature, even in suspension; this was the foundation for preparing FBPAs.

1.2. Synthesis of FBPAs. Fluorescent dye coupling to PFPE takes advantage of the high reactivity of PFPE ester 1 toward primary amines. The polymeric nature and high lipophobicity of PFPE ester 1 complicates the conjugation reaction to a lipophilic dye, such as BODIPy-TR. The BODIPy-TR used already had cadaverine (1,5-diaminopentane) conjugated to one end, leaving an unmodified amine free for further coupling. PFPE ester 1 is fully soluble only in trifluoroethanol, trifluorotoluene and perfluorohexanes. Trifluoroethanol was the only solvent that solubilizes both the dye and the PFPE oil. BODIPy-TR cadaverine was added at low concentration (5 mg dye/1 mL of PFPE oil) and allowed to react for 48 h at r.t. in trifluoroethanol. All unreacted PFPE ester end groups are converted to tertiary diethyl amides (Scheme 2). The coupling yield of BODIPy-TR cadaverine to PFPE was 46.8% (i.e., final content in PFPE 0.6 mol %), as estimated from absorbance measurements of fluorophilic and fluorophobic fractions after fluorous silica gel filtration.

Our synthetic approach for fluorescent PFPEs relies on the highly efficient initial coupling of the primary amine of the fluorescent dye conjugate to PFPE ester 1. This assumption is

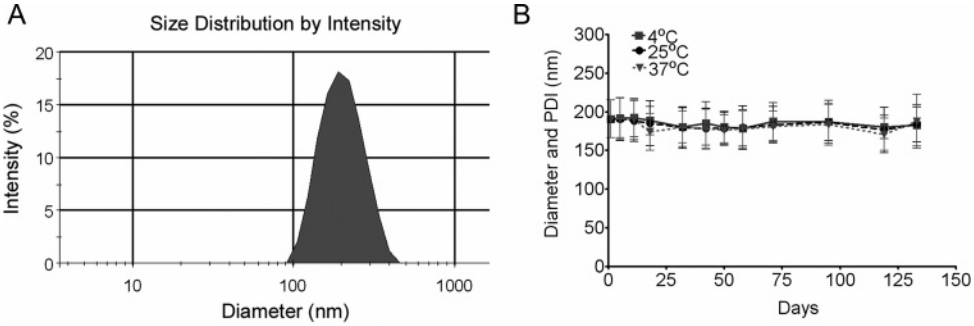

Figure 1. DLS analysis of BODIPy-TR PFPE nanoemulsion. Panel A displays the diameter distribution by light intensity, and B shows diameter and PDI (error bars) followed over time at three different storage temperatures: 4 (■), 25 (●), and 37 °C (▼).

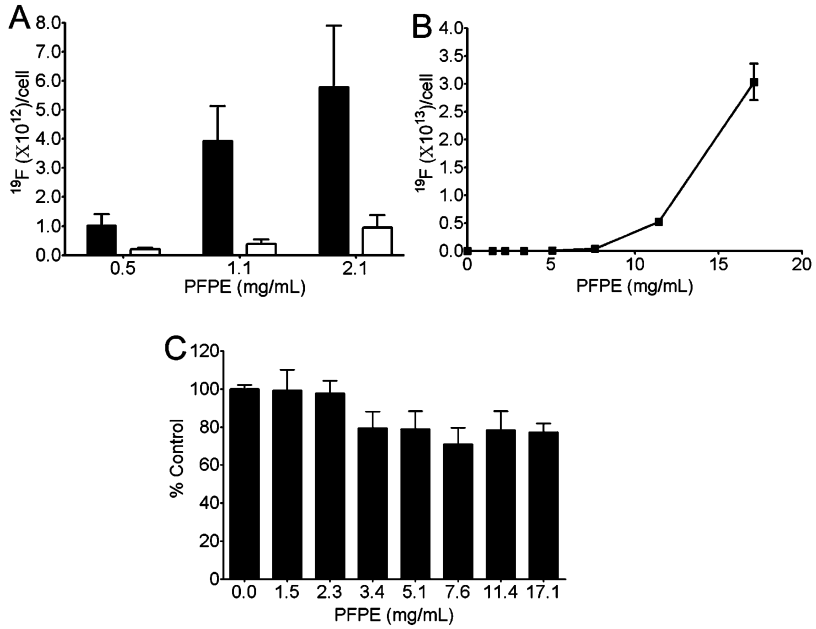

Figure 2. BODIPy-TR PFPE nanoemulsion uptake in Jurkat cells and viability post-labeling. (A) Effect of PEI on PFPE uptake, where solid and open bars are PFPE nanoemulsion with and without PEI, respectively; (B) dose dependent PFPE nanoemulsion uptake in Jurkat cells; (C) Cell viability post-labeling. Each data point in panels A−C represents the average of three independent measurements, where the error bars are the standard deviation of the mean.

based on the model reaction described above, Scheme 1, where complete conversion (>99%) is observed by ^{1}H NMR after 48 h at r.t. The final product is FBPA, a perfectly blended mixture of PFPE derivatives comprised of dye di-conjugate 5, dye mono-conjugate 6 and PFPE amide 2 (Scheme 2). The FBPA was used for fluorescent PFPE nanoemulsion preparations by further blending with PFPE oxide (Perfluoropoly(ethylene glycol) dialkyl ether, Exfluor Inc., TX)[33] (Chart 1). We demonstrate that PFPE amides are stable and hold the fluorescent dye in the PFPE oil phase during microfluidization. Fluorescence measurements show the BODIPy-TR dye spectrum is unchanged after coupling to PFPE (Supporting Information, Figure 1).

1.3. PFPE Nanoemulsion Preparation by Microfluidization. Fluorescent PFPE nanoemulsions were prepared from PFPE oils (FBPA and PFPE oxide) using high shear microfluidization[34] with F68 and PEI in deionized water. Chart 1 shows structures of all nanoemulsion components.

PFPE oils, FBPA and PFPE oxide were first blended together by continuous vortexing on the highest speed for 5 min, followed by mixing with F68 and PEI water solutions and then microfluidized. High mechanical energy applied within the interaction chamber of the microfluidizer disperses PFPE hydrophobic oil in water and results in monodisperse nanoemulsions. Nonfluorescent PFPE nanoemulsions were prepared by mixing PFPE oxide and PFPE amide 2 at a ratio 9/1 v/v. Fluorescent nanoemulsions were prepared from PFPE oxide and FBPA at 9/1 v/v ratio. All nanoemulsions were filter-sterilized (PTFE filter, pore size 0.22 μm) and stored at 4 °C until use for cell labeling.

1.4. Fluorescent PFPE Nanoemulsion Characterization and Stability. Fluorescent PFPE nanoemulsions were characterized by ^{19}F NMR (470 MHz) and dynamic light scattering (DLS) measurements (Zetasizer Nano, Malvern, UK). The main peak (−91.58 ppm) in the ^{19}F NMR spectrum of the final fluorescent PFPE nanoemulsion diluted in dionized water shows no change in chemical shift as compared to the spectrum of the neat PFPE oil (Supporting Information Figure 3). The main component of the PFPE oil in the nanoemulsion droplet is PFPE oxide (at 90% v/v), with the remaining being FBPA. The minor peaks in the ^{19}F NMR spectrum (Supporting Information Figure 3) represent known chemical shifts for the PFPE oxide.[33]

The average droplet size for all fluorescent nanoemulsions, measured by DLS, was 160−190 nm, with a low polydispersity index (PDI) of <0.15. Figure 1A shows the size distribution of

(33) Gerhardt, G. E.; Lagow, R. J. *J. Org. Chem.* **1978**, *43*, 4505−4509.
(34) Sorgi, F. L.; Huang, L. *Int. J. Pharm.* **1996**, *144*, 131−139.

BODIPy-TR PFPE nanoemulsion in water as measured by DLS at room temperature. The symmetric shape of the graph indicates spherical droplets. The presence of fluorescent dyes in PFPE oils had virtually no effect on the emulsification, particle size, polydispersity, or shelf life.

Serum stability was tested for all emulsions by adding nanoemulsion into 10% (v/v) FBS in RPMI at 37 °C for 24 h. Nanoemulsions prepared with BODIPy-TR and FITC PFPE conjugates were observed to be stable in the presence of serum, showing no change in average droplet size or PDI. However, in the presence of serum the Alexa647 containing PFPE nanoemulsion showed an increase in particle size by ~30% after only 3 h. The presence of anions in the Alexa647 dye structure was the likely cause of the emulsion degradation, which was accelerated by the presence of proteins in the serum.

Shelf life of reported PFPE nanoemulsions was evaluated by repeated DLS measurements. Stability was tested for at least 5 months for emulsions stored at 4, 25 and 37 °C. No significant variation in diameter or PDI was observed over time at all three storage temperatures, Figure 1B. Due to its robust shelf life and photo and chemical stability, BODIPy-TR PFPE was used for all in vivo experiments.

2. Cell Labeling with Fluorescent PFPE Nanoemulsions. Cell labeling using the nanoemulsions was demonstrated in both phagocytic cells, using a fetal-skin derived mouse DC line,[18] and in non-phagocytic cells, including primary T cells and Jurkat cells. In all cell types studied, suitable levels of emulsion uptake for in vivo MRI (i.e., $>10^{11}$ ^{19}F/cell) were achieved in a modest 3 h incubation period. Intracellular localization of the nanoparticles was visualized using fluorescence microscopy. Cellular uptake of nanoemulsion droplets was quantified using fluorescence measurements and by ^{19}F NMR spectroscopy of lysed cell pellets. Uptake was tested by ^{19}F NMR, where the PFPE labeled cells show a major peak at −91.58 ppm; the −76.00 ppm peak is from TFA reference added to lysed cell pellet. The integrated areas under these two peaks can be used to calculate the mean ^{19}F/cell (see Supporting Information), often ranging from 10^{11}−10^{13}. The same approach was used for evaluating uptake in all cell types tested.

2.1. BODIPy-TR PFPE Nanoemulsion Concentration Dependent Cellular Uptake. Jurkat cells, an acute T cell leukemia perpetual line, were used as a model cell line to evaluate PFPE nanoemulsion uptake in cells grown in suspension. These cells express a T cell receptor and can proliferate under similar cell culturing conditions as T cells.[35]

Jurkat cells do not have phagocytic abilities and thus served as an excellent model to evaluate the effects of PEI on the PFPE nanoemulsion uptake. To label cells, PFPE nanoemulsion was simply added to the culture medium and incubated for 3 h at 37 °C. Cells were washed and then examined for viability and PFPE nanoemulsion uptake. Primary amines from PEI in PFPE nanoemulsions were necessary for Jurkat cell labeling as shown in Figure 2A. PFPE nanoemulsion without PEI shows dramatically decreased uptake in Jurkat cells. PEI was also necessary for a concentration dependent labeling of Jurkat cells (Figure 2B). For all PFPE concentrations tested, cell viability was >70% compared to the untreated control (Figure 2C). Following labeling, Jurkat cell proliferation was no different then untreated cells (data not shown), and no changes in cell morphology were observed by light microscopy. The cells appeared healthy and unaffected by even the highest doses of PFPE nanoemulsions tested.

2.2. BODIPy-TR PFPE Nanoemulsion Cell Labeling in Phagocytic and Adherent DCs. A mouse DC line was used to test nanoemulsion uptake in a phagocytic and adherent cell type. The cells were collected after 3 h incubation with BODIPy-TR PFPE nanoemulsion; the typical ^{19}F NMR spectrum of labeled cells is shown in Figure 3A. Cellular uptake (^{19}F/cell) and dose response is comparable to what is observed for Jurkat cells in Figure 2B (data not shown).

The intracellular distribution of the BODIPy-TR PFPE nanoemulsion droplets in DCs was investigated using fluorescence microscopy (Figures 5B−D). The cell surface was labeled with anti-CD45 FITC conjugated antibody and nuclei were stained with Hoechst 33342 dye (Invitrogen, Carlsbad, CA). The BODIPy-TR PFPE nanoemulsion appeared evenly distributed throughout the cytoplasm inside vesicle-like formations. This finding is consistent with previous reports[18] showing that PFPE nanoparticles concentrate in subcellular vesicles within DCs. No co-localization of the fluorescent PFPE nanoemulsion droplets with cell membranes was observed (Figure 5B, Supporting Information Figure 5).

2.2. Primary Mouse T Cell Labeling: ^{19}F NMR, Fluorescence Microscopy and FACS Analysis. Primary T cells were isolated from the mouse spleen as previously described.[19] Cells were activated by IL-2 for 3 days prior to BODIPy-TR PFPE nanoemulsion labeling. The cell viability was >86% compared to control cells, as determined by the trypan blue exclusion assay 5 h post-labeling. Figure 4A shows a typical ^{19}F NMR spectrum of PFPE labeled T cells (2×10^6), where the −91.58 ppm peak is the labeled cells and the TFA is at −76.0 ppm. Labeled T cells were visualized by fluorescence microscopy. Figure 4B-C shows the T cell surface (green) labeled with anti-CD4-FITC antibody and the BODIPy-TR PFPE nanoemulsion (red), for panels B and C, respectively. Confocal microscopy clearly shows cytoplasmic localization of the PFPE nanoemulsion within T cells (Figure 4E). Additional confocal microscopy images of BODIPy-TR PFPE labeled T cells are available in the Supporting Information.

The phenotype of the labeled T cells was evaluated by two-color FACS analysis. Figure 5 shows that activated T cells express normal levels of the cell surface markers CD4 and CD25. The majority of T cells were dual-positive, showing red BODIPy-TR PFPE and green CD4-FITC or CD25-FITC. The surface marker expression levels (Figure 5E,F) were unchanged as compared to untreated control (Figure 5B,C).

3. ^{19}F NMR Signal−Fluorescence Correlation. A calibration curve was generated from serial dilutions of BODIPy-TR PFPE emulsion (0−11.4 mg PFPE per mL) that were placed in 96-well plates in triplicate (0.20 mL/well). Fluorescence was measured at fixed wavelengths (550 nm excitation and 625 nm emission). The same dilutions were also measured by ^{19}F NMR at 470 MHz, and the number of ^{19}F per well was estimated using the −90.58 ppm peak with respect to the TFA reference. A plot of the ^{19}F signal versus the fluorescence displays a linear correlation with $r^2 = 0.982$ and $p < 0.0001$ (Figure 6A). To test whether this linearity holds for labeled cells, Jurkat cells were labeled with BODIPy-TR PFPE nanoemulsion for 3 h, and fluorescence and ^{19}F NMR measurements were performed

(35) Gillis, S.; Smith, K. A.; Watson, J. *J. Immunol.* **1980**, *124*, 1954−1962.

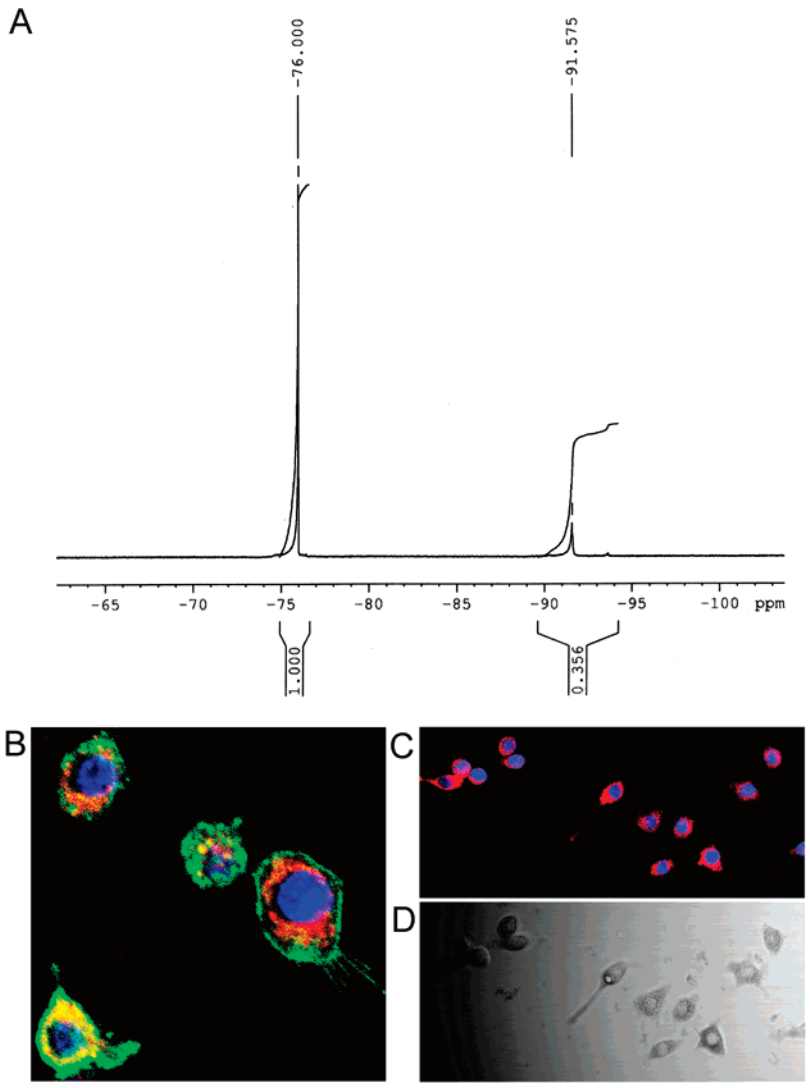

Figure 3. Mouse DCs labeled with BODIPy-TR PFPE nanoemulsion. (A) Shows a ^{19}F NMR spectrum of labeled DCs (−91.58 ppm) and TFA (−76.00 ppm) reference. Panels B−C display fluorescence micrographs of BODIPy-TR PFPE nanoemulsion in the cytoplasm (red), Hoechst 33342 labeled nuclei (blue) and the CD45-FITC labeled cell surface (green). (D) DIC image of labeled DCs.

in triplicate. The measured signals for each modality, the relative fluorescence units (RFU) and area under the −91.58 ppm peak in the ^{19}F NMR spectrum, were normalized by the total cell number per sample. The results display a linear correlation with $r^2 = 0.983$ and $p < 0.0001$ (Figure 6B). Importantly, the linearity between fluorescence and ^{19}F NMR signal in cells demonstrates the utility of fluorescence detection for quantification of in vitro cell loading of the ^{19}F MRI tracer agent.

4. MRI of T Cells in Vivo Labeled with BODIPy-TR PFPE Nanoemulsion. To demonstrate that the dual mode reagent is effective for in vivo MRI studies, we used a simple cell transfer model utilizing female BALB/c mice as both a donor and recipient. Primary, naïve T cells were harvested from a donor animal, and labeled the same day as described above. Labeled cells (1×10^7) were injected into the recipient mouse via an intraperitoneal (i.p.) injection. ^{1}H and ^{19}F MRI was carried out 2 days after cell transfer using an 11.7 T micro-imaging system. Figure 7 shows the distribution of BODIPy-TR PFPE nanoemulsion-labeled naïve T cells in the mouse torso; the image shows several punctate spots that are presumed to be lymph nodes, possibly the hepatic, mesenteric, and periaortic lymph nodes. The majority of transferred cells are in other tissues or in circulation at concentrations too low to be detected by MRI. The trafficking of PFPE labeled naïve T cells preferentially to lymph nodes is expected and consistent with previous studies.[36] Similarly prepared T cells were evaluated in detail by fluorescence microscopy (Figure 4) and FACS analysis (Figure 5).

To confirm the MRI findings and to demonstrate the duality of the BODIPy-TR PFPE nanoemulsion, FACS analysis, and fluorescence microscopy were performed on cells isolated from various lymph nodes post-imaging. The mice were sacrificed and the lymph nodes showing positive ^{19}F signal by MRI were surgically isolated, and the cells were processed for FACS and microscopy analysis. In these cells, we were able to detect CD4+ cells that retained BODIPy-TR PFPE for several days post-injection. The FACS and microscopy data is available in the Supporting Information (Figures 6 and 7).

Discussion

We report an efficient and scalable synthetic method for preparing stable, nontoxic fluorescently labeled fluorinated nanoemulsions for dual ^{19}F MRI-fluorescence detection. We

(36) Williams, M. B.; Butcher, E. C. *J. Immunol.* **1997**, *159*, 1746−1752.

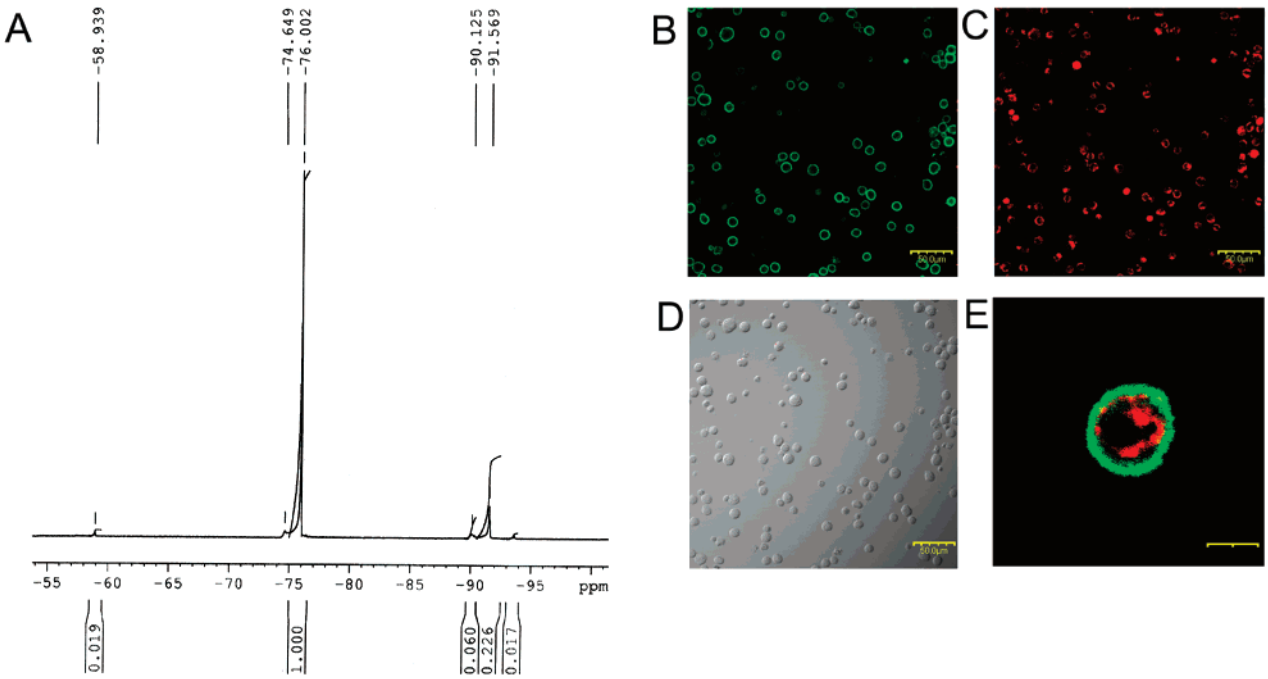

Figure 4. Mouse primary activated T cells labeled with BODIPy-TR PFPE nanoemulsion. (A) ^{19}F NMR spectrum of labeled T cells, TFA (−76.00 ppm) reference and cells (−91.58 ppm); (B−D) Labeled T cells stained with CD4-FITC (green) antibody. Scale bar is 50 μm; (E) Confocal image of labeled T cells showing cytoplasmic localization of nanoemulsion post-labeling (red) and the CD4-FITC labeled cell surface (green). Scale bar is 20 μm.

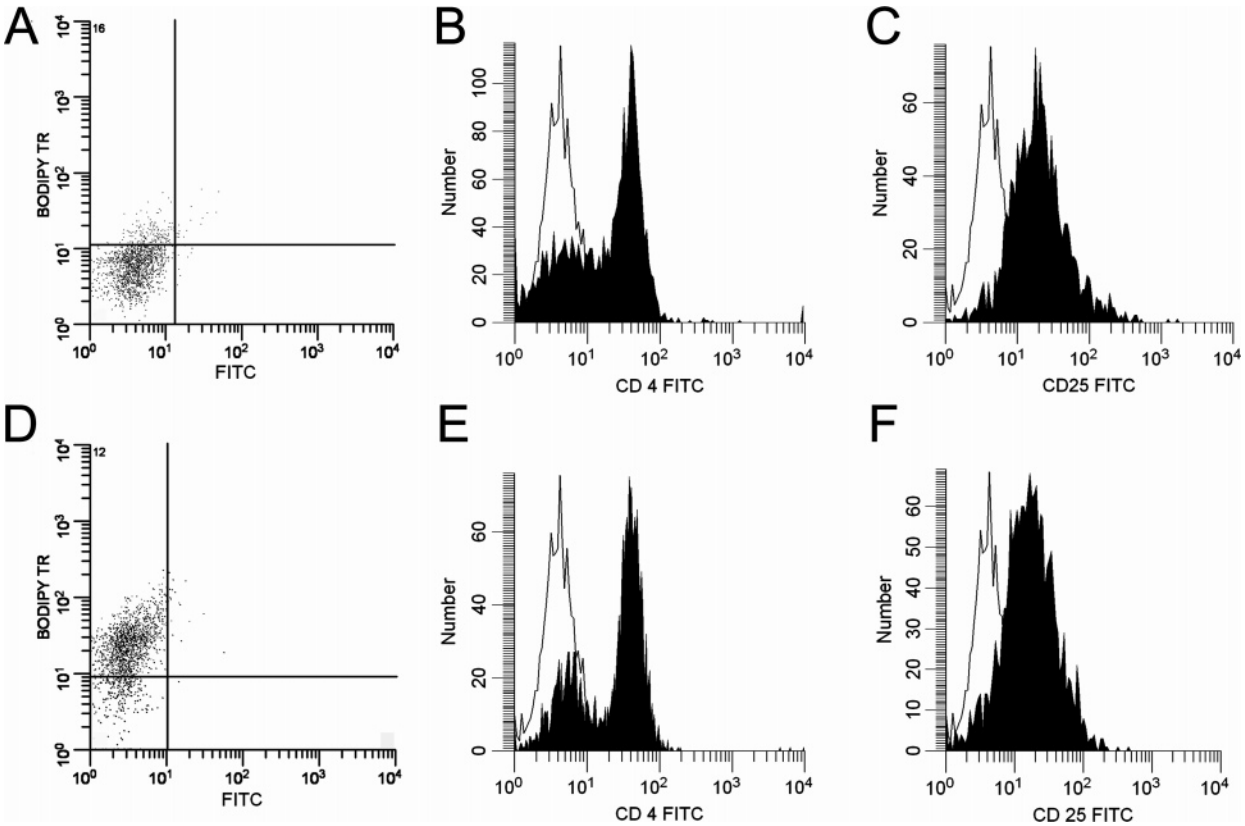

Figure 5. FACS analysis of activated, mouse primary T cells labeled using BODIPy-TR PFPE nanoemulsion T cells. (A) Untreated T cells. (B) Untreated T cells stained with CD4-FITC antibody (filled) overlaid with IgG-FITC control. (C) Untreated T cells labeled with CD25-FITC antibody (filled) overlaid with IgG-FITC control. (D) BODIPy-TR PFPE nanoemulsion labeled T cells. (E) BODIPy-TR PFPE nanoemulsion labeled T cells stained with CD4-FITC antibody (filled) overlaid with IgG-FITC control. (F) BODIPy-TR PFPE nanoemulsion labeled T cells stained with CD25-FITC (filled) overlaid with IgG-FITC control.

demonstrate that PFPE ester 1 is a versatile starting material for the synthesis of PFPE nanoemulsions. These nanoemulsions exhibit highly efficient uptake in both phagocytic and non-phagocytic cell types. Presented nanoemulsions are stable at storage temperatures (4 and 25 °C) and body temperature (37 °C) for several months, showing no change in droplet size (160−

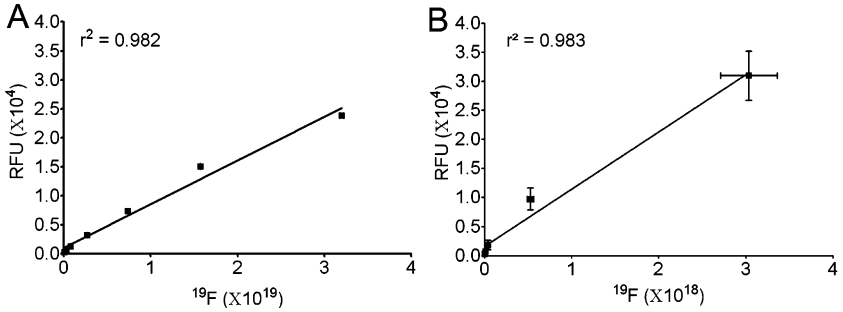

Figure 6. ^{19}F NMR signal-fluorescence correlation. Panel A shows nanoemulsion dilutions in water and B displays nanoemulsion labeled Jurkat cells. Each data point represents an average of three independent measurements, where the error bars are the standard deviation. In A, the error bars are within the symbols.

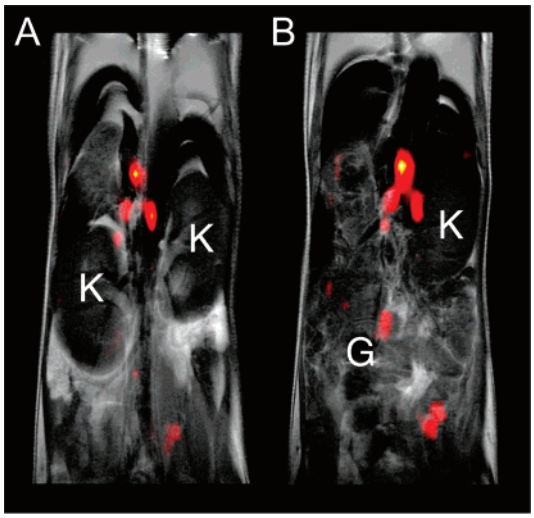

Figure 7. In vivo MRI of labeled T cells in the mouse model. The ^{19}F image (pseudo-color) shows a localized accumulation of T cells labeled with PFPE nanoemulsion in lymph nodes and the grayscale underlay is an anatomical ^{1}H image. Panels A and B display two consecutive 2-mm thick slices through the torso, and for anatomical orientation the kidneys (K) and gut (G) are noted. During imaging, the mouse was anesthetized with a ketamine/xylazine cocktail, connected to a mechanical ventilation apparatus, acquisitions were cardio-respiratory gated, and body temperature was regulated at 37 °C. Data were collected for both ^{19}F and ^{1}H in a single imaging session.

190 nm) and PDI (<0.15). BODIPy-TR PFPE nanoemulsion were used to ex vivo label naïve mouse T cells that were then administered in vivo to a simple BALB/c mouse model and imaged by ^{19}F MRI. The cells accumulated in regions consistent with the mesenteric, hepatic, and periaortic lymph nodes. The dual-mode nanoemulsions presented here enable a powerful range of cell characterizations using fluorescence-based cytometry or histology of biopsied tissue. The lymph nodes showing the most intense ^{19}F signal were surgically isolated post-imaging, a single cell suspension was prepared, and FACS analysis and microscopy confirmed the presence of fluorescent nanoemulsion in viable CD4 positive T cells (see Supporting Information). Importantly, the magnitude of the fluorescence signal in a known cell population can be used to calibrate the extent of nanoemulsion loading into cells ex vivo prior to animal transfer using simple fluorimeter instrumentation.

Prior art labeled DCs for in vivo ^{19}F MRI used an emulsified perfluoro-15-crown-5-ether molecule.[18,20] In the present study, we have chosen a linear PFPE molecule that contains a larger number of NMR-equivalent ^{19}F nuclei per molecule for high sensitivity. For the linear PFPE, the ^{19}F spins from the CF_2-CONH and CF_3 end groups produce signal that is below the detection limit of in vivo MRI acquisitions, having approximately 10× lower intensity than the main peak from CF_2-CF_2O repeats. In addition, the ^{19}F T1 = 437 ms of the CF_2 in the monomer units (CF_2CF_2O) of linear PFPE molecule is 2.2× shorter than the T1 at 11.7 T of perfluoro-15-crown-5-ether CF_2 resonance, thus permitting proportionally shorter imaging times. The linear PFPE does not readily coordinate O_2 as does the perfluoro-15-crown-5-ether, and hence it is less sensitive to T1 changes due to local differences in the partial pressure of O_2. Furthermore, a major challenge of perfluoro-15-crown-ether for MRI probe development is its chemical inertness, which does not permit further modifications without destroying the unique symmetry that gives a single ^{19}F NMR resonance. In the large linear PFPE polymer, the CF_2CF_2O unit repeats give rise to one major peak at −91.58 ppm and linear PFPE is amendable to chemical modification; for example, linear PFPE ester 1 allows for conjugation to a variety of fluorescent dyes.

PFPEs are highly hydrophobic and lipophobic, with limited solubility in common organic solvents but soluble in fluorinated solvents such as trifluorotoluene, trifluoroethanol and perfluorohexanes. The alkyl ester end groups of PFPE esters hydrolyze very easily in neutral, acidic and basic media and are highly reactive toward various nucleophiles.[28] PFPE esters can easily react with primary and secondary amines without additional ester activation, due to the increased nucleophilicity of the carbonyl by the electron withdrawing effect of neighboring fluorines. Previous reports demonstrated the coupling of amines to PFPE alkyl esters under elevated temperature.[37] We report the same coupling under mild conditions, room temperature, and with limited or no solvent. The PFPE ester coupling to primary amines is also possible by performing the reaction in suspension, where the amine (solid) is suspended in the PFPE ester (oil). This high reactivity of PFPE ester groups toward primary amines was exploited in the preparation of fluorescently labeled PFPE oils. BODIPy-TR, FITC, and Alexa647 cadaverine monoconjugates were coupled via secondary amide bond to PFPE, producing highly fluorescent PFPE oils (e.g., FBPAs). The fluorescent dye, while covalently bound to PFPE, remains with the rest of PFPE oil. PFPE behaves as fluorous phase[32] in this final product. Therefore, all PFPE derivatives are easily blending with each other. In the final product, several PFPE derivatives behave as continuous fluorocarbon oil. These blended PFPE oils were composed of 0.5−2.0 mol % of fluorescent dye conjugated to PFPEs 5 and 6 and 98.0−99.5 mol % of PFPE

(37) Piacenti, F.; Camaiti, M. *J. Fluorine Chem.* **1994**, *68*, 227−235.

Chart 2. Preparation of the Fluorescent PFPE Nanoemulsion by Microfluidization[a]

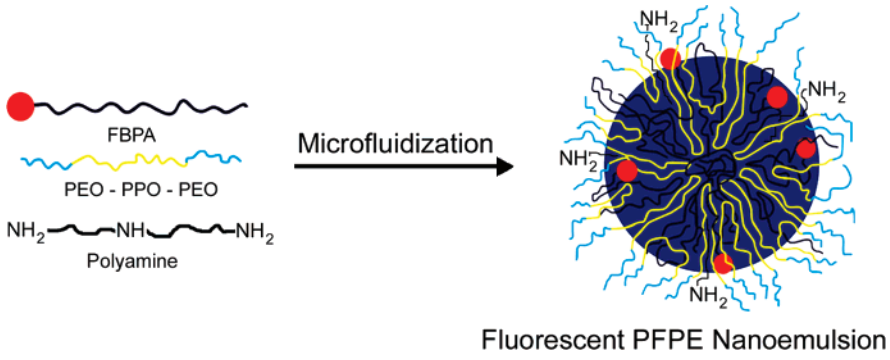

[a] Fluorescent Dye Is BODIPy-TR, FITC, or Alexa647.

amide 2, Scheme 2. The boradiazaindacene family (BODIPy) of fluorescent dyes have moderate extinction coefficients and quantum yields, but have higher photo and chemical stability compared to other common dyes such as fluorescein and rhodamine.[38] BODIPy fluorescence is insensitive to the environment, which enables them to be an attractive candidate for nanoemulsion preparations by high shear based methodologies. In nanoemulsion preparations, Alexa647 and FITC conjugates initially gave similar results, however, the Alexa647 fluorescence diminished after approximately 1 month storage at temperatures 25 and 37 °C. Most of the biological data reported here were obtained from using nanoemulsions containing BODIPy-TR PFPE amide FBPA. These fluorescent oils were comparable in their emulsification properties against nonfluorescent PFPEs.

Nanoemulsions are kinetically stable emulsions with a droplet size typically between 20 and 500 nm. Unlike microemulsions, which can form spontaneously, nanoemulsions require high-energy processing, such as microfluidization or sonication. Due to the small droplet size, nanoemulsions are translucent and typically resistant to creaming and sedimentation. Nanoemulsion formation usually does not require high amounts of surfactant, and nanoemulsions can be stabilized by steric effects.[39] General practical and theoretical considerations for preparation of stable nanoemulsions are reviewed elsewhere.[40]

We used two emulsifiers in the formation of the nanoemulsions, which included pluronic F68 and linear, low molecular weight PEI. A novel aspect of this work is the use of PEI as a coemulsifier along with pluronic to prepare fluorocarbon nanoemulsion in water. Pluronic F68 is a nontoxic, nonionic block copolymer that is FDA approved for human applications. F68 has been used with egg yolk lecithin for emulsification of perfluorocarbons in blood substitute formulations; F68 stabilized the fluorocarbon oil droplets in aqueous external phase by steric effects.[41] Previous structural studies of fluorocarbons emulsified with block polymers, showed that the block polymer was adsorbed at the interface between the colloid fluorocarbon and the aqueous media.[42−44] The nanoemulsion droplet structure reported here is presented in Chart 2, where the fluorinated polymer (PFPE) core is coated with a thin film of F68 mixed with PEI. Because PFPE is both hydrophobic and lipophobic, we hypothesize that the particles are oil droplets coated with F68 and PEI and are presumed to be stabilized by steric effects of the block polymer polyethylene oxide (PEO) portion.

The hydrophilic fluorescent dyes Alexa647 or FITC are likely closer to the surface; in contrast, non-ionizable and lipophilic BODIPy-TR dye is likely to be buried deep into the pluronic block polymer, i.e., PEO-PPO-PEO, lipophilic layers (polypropylenoxide, PPO). In order to facilitate nanoemulsion delivery into cells, PEI was added to the emulsion preparation. PEI is a polyamine transfection agent known to help DNA, RNA or proteins enter into cells.[45] Linear PEI (MW ≈ 430) was not coupled directly to PFPE, but incorporated into the emulsion during processing to supply nanoemulsion droplets with primary and secondary amine groups to promote cellular uptake. Branched, high molecular weight PEI (MW ≈ 25 000) has been often used for efficient cellular DNA delivery. Linear, low MW PEI is not as efficient delivery agent on its own,[46] but is far less toxic to cells. When PFPE was emulsified with pluronic alone, the uptake was too low to be useful for MRI-based cell tracking in non-phagocytic cell types ($<10^{10}$ ^{19}F/cell). PFPE nanoemulsions prepared with PEI had dramatically increased cell labeling potency in non-phagocytic Jurkat cells, as shown in Figure 2A.

Successful and optimal cell labeling with PFPE nanoemulsions is affected by droplet size, PDI, and emulsion stability in cell culture media. When cells are mixed with emulsion droplets, small droplet size and PDI results in a homogeneous distribution of nanoemulsion in the culture media. Thus, each cell is uniformly exposed to a large number of PFPE droplets that facilitates consistency in cell labeling. With too large a droplet, there is a possibility for sedimentation and aggregation during cell labeling. Importantly, large droplets confound the centrifugation cell washing steps post-labeling because large emulsion particles will spin down with the cells. We have empirically observed that a particle size below ∼200 nm avoids these problems. We also tested emulsion stability in presence of serum and found the emulsions were stable with prolonged incubation (up to 24 h) under cell labeling conditions. In practical terms,

(38) Haughland, R. P. *Handbook of Fluorescent Probes and Research Products*, 9 ed.; Spence, M. T. Z., Ed.; Molecular Probes Inc.: Eugene, OR, 2002.
(39) Forgiarini, A.; Esquena, J.; González, C.; Solans, C. *Langmuir* **2001**, *17*, 2076−2083.
(40) Tadros, T.; Izquierdo, P.; Esquena, J.; Solans, C. *Adv. Colloid Interface Sci.* **2004**, *108*−*109*, 303−318.
(41) Hsu, L.-C.; Creech, J.; Zalesky, P.; Kivinski, M. 2004, US 2004/57906 A1.
(42) Washington, C.; King, S. M.; Attwood, D.; Booth, C.; Mai, S. M.; Yang, Y. W.; Cosgrove, T. *Macromolecules* **2000**, *33*, 1289−1297.
(43) Washington, C.; King, S. M. *Langmuir* **1997**, *13*, 4545−4550.
(44) Washington, C.; King, S. M.; Heenan, R. K. *J. Phys. Chem.* **1996**, *100*, 7603−7609.
(45) Godbey, W. T.; Wu, K. K.; Mikos, A. G. *J. Controlled Release* **1999**, *60*, 149−160.
(46) Thomas, M.; Ge, Q.; Lu, J. J.; Chen, J.; Klibanov, A. M. *Pharm. Res.* **2005**, *22*, 373−380.

a dual-mode fluorescent-^{19}F MRI agent is particularly valuable for calibrating the in vitro intracellular dose post-labeling of the MRI agent using quantitative fluorescence imaging as a substitute for costly ^{19}F NMR. Most clinical and biomedical research laboratories have access to fluorescent plate readers, but ^{19}F-capable NMR instrumentation is much less common.

Conclusion

In summary, we have synthesized unique fluorescent perfluorocarbon nanoemulsions that efficiently label non-phagocytic cells, such as lymphocytes (T cells, Jurkat cells) and phagocytic cells (DCs) for in vivo cell tracking by ^{19}F MRI. The nanoemulsions are easy to use and efficiently label diverse cell types without addition of transfection reagents or cationic lipids. The cellular uptake can be measured by fluorescence as an alternative to ^{19}F NMR. We demonstrate a linear correlation between fluorescent signal and ^{19}F NMR peak intensity in labeled cells. Overall, we envision that PFPE labeling is widely applicable to a range of in vivo cell trafficking studies in both the discovery and preclinical setting. The addition of a robust fluorescent tag to unambiguously characterize transferred cells greatly complements in vivo MRI cell trafficking studies.

Acknowledgment. The authors thank Robert Gibbs for help with fluorescence microscopy, E. Michael Meyer for help with FACS analyses, Billy W. Day for providing MALDI-TOF analyses, and Kevin Hitchens for helpful comments. This work was funded in part by the National Institutes of Health (R01-EB003453, R01-EB004155, and P01−HD047675). The Pittsburgh NMR Center is supported by the National Institute of Biomedical Imaging and Bioengineering as a National Biomedical Research Resource Center (P41EB-001977).

Supporting Information Available: Experimental methods including synthesis of fluorescent PFPE oils, nanoemulsion preparation and biological testing, and experimental analysis: fluorescence, FACS analysis, confocal microscopy, UV/VIS, NMR (^{1}H, ^{19}F, ^{13}C) and MS characterization data for select compounds. This material is available free of charge via the Internet at http://pubs.acs.org.

JA077388J